International Journal of Heat and Mass Transfer 53 (2010) 2943–2950

Contents lists available at ScienceDirect

International Journal of Heat and Mass Transfer

journal homepage: www.elsevier.com/locate/ijhmt

# Synthesis of biofilm resistance characteristics against antibiotics

Maryam Shafahi, Kambiz Vafai *

*Department of Mechanical Engineering, University of California, Riverside, Riverside, CA 92521, USA*

ARTICLE INFO

*Article history:*
Received 2 January 2010
Received in revised form 6 March 2010
Accepted 6 March 2010
Available online 21 April 2010

*Keywords:*
Bacterial transport
Biofilm resistance
Antibiotic
Disinfection
*Pseudomonas aeroginosa*
Microbial survival

ABSTRACT

A phenomenological model for the biofilm resistance against biocide activity is analyzed in this work. The effect of different biofilm physical attributes when exposed to antibiotic treatment is investigated. Pertinent aspects affecting the biofilm resistance characteristics such as transport of the bulk fluid within the reactor, diffusive-reactive transport of the dissolved phase into the biofilm, convective-reactive transport of particulate phase, dynamic biofilm thickness, cell detachment, extracellular polymeric substance (EPS) production and persister cell formation are analyzed and incorporated in the presented model. Microbial survival fraction is correlated in terms of pertinent non-dimensional groups from biofilm and bulk fluid governing equations and the effect of persister cell formation on the biofilm response to biocide disinfection is demonstrated. To the authors' best knowledge, the current model is the first comprehensive model that considers several physical attributes simultaneously and presents a set of correlations to predict the microbial survival of a biofilm subject to the biocide treatment.

© 2010 Elsevier Ltd. All rights reserved.

## 1. Introduction

Biofilms are heterogeneous conglomerate of microorganisms which play a significant role in causing different diseases. National Institute of Health announcement shows that over 80% of microbial infections in the body are related to biofilms [1,2]. Many persistent and chronic infections such as endocarditis, osteomyelities, periodontitis, otitis media and biliary tract infections have been connected to the presence of biofilms. Biofilms can also result in or extend infections through colonization of implants or prosthetic devices [3–7]. Although antibiotics are the most common tools to eradicate bacteria, they are not efficient enough to remove them in the presence of the biofilms [8]. Analyzing the biocide delivery attributes can lead to an optimized treatment. A number of works have been published on modeling the biofilm resistance against antibiotics [1,9–16].

Different approaches have been utilized to explain the decrease in biocide efficiency inside bacterial biofilms. In some of these works [17–19], it is assumed that either a neutralizing reaction occurs inhibiting the antibiotics efficiency within the film or that there is a barrier against penetration [20]. The other limiting factors for biocide transport are related to a degrading enzyme produced by bacteria [21–22] and adsorption in extracellular polymeric substance (EPS) [23]. It has been mentioned that the biofilm's exopolysaccharide protects the bacteria against the immune system [24,25]. Microbial growth rate has a significant effect on the survival fraction of the bacteria. A wide range of cells from fast growing to dormant can exist inside the biofilms [26–28]. Generally, the faster growing cells will die more readily when exposed to a proper antibiotic [7,20]. For most cases, nutrient and antibiotic concentrations decrease and microbial cell survival fraction increases in going from bulk interface towards substratum within the biofilm. As a result, the efficacy of an antibiotic is reduced in moving from the interface to the deeper layers of the biofilm. The reaction terms for both the particulate and dissolved phases incorporate this trend. It has been shown that for some cases neither transport limitation nor physiological heterogeneity were able to explain the reduced susceptibility of the biofilm to an antibiotic treatment [1,26,29]. A relatively new idea in explaining the biofilm's resistance against antibiotics is the formation of extremely resistant cells, called persisters, within the film. A number of experimental and theoretical investigations have been done exploring the existence of these types of cells [1,2,13,20,29,30].

In the present work, a pertinent multispecies biofilm model, a modified version of the model presented in Shafahi and Vafai [31], is utilized to analyze the changes normal to the substratum. The biofilm structure is considered as a porous medium [32–34] and EPS production is included in the reaction terms based on Wanner et al. model [35]. The resistance model is examined for *Pseudomonas* aeuroginosa (Pa) biofilm exposed to Piperacillin and results are compared with available experimental data. Survival fraction curves show the difference between the biofilm response with and without the formation of persister cells.

The aim of this study is to analyze the influence of pertinent factors such as nutrient and biocide diffusion, cell infection, cell growth and convection, persister cell formation and attachment and detachment in the bulk fluid on the biofilm survival characteristics. In order to clarify the biofilm's characteristics subject to bio-

* Corresponding author. Tel.: +1 951 827 2135.
*E-mail address:* vafai@engr.ucr.edu (K. Vafai).

0017-9310/$ - see front matter © 2010 Elsevier Ltd. All rights reserved.
doi:10.1016/j.ijheatmasstransfer.2010.04.004

**Nomenclature**

| | |
|---|---|
| $A$ | surface area ($m^2$) |
| $B$ | dimensionless group |
| $C$ | concentration ($g/m^3$) |
| $D$ | diffusion coefficient ($m^2$/day) |
| $i_1$ | stoichiometric coefficient ($g_C/g_{O2}$) |
| $i_2$ | stoichiometric coefficient ($g_{pa}/g_{EPS}$) |
| $k$ | reaction coefficient ($g/m^3$/day) |
| $k_d$ | disinfection rate coefficient ($m^3$/g/day) |
| $k_{lo}$ | loss rate coefficient |
| $K$ | Monod coefficient ($g/m^3$) |
| $L$ | biofilm thickness (m) |
| $Q$ | volumetric flow rate ($m^3$/day) |
| $r$ | reaction term ($g/m^3$/day) |
| $s_n$ | survival fraction without persister cells |
| $s_p$ | survival fraction with persister cells |
| SRS | square root of survival |
| $t$ | time (day) |
| $t_b$ | treatment duration (day) |
| $u$ | velocity (m/day) |
| $u_l$ | biofilm interface velocity (m/day) |
| $Y$ | yield coefficient |
| $Y_{Pa/glu}$ | cell yield coefficient ($g_{Pa}/g_{glu}$) |
| $Y_{EPS/glu}$ | EPS yield coefficient ($g_{EPS}/g_{glu}$) |
| $W$ | correlation coefficient |
| $x$ | normal coordinate |

*Greek symbols*

| | |
|---|---|
| $\varepsilon$ | porosity |
| $\varepsilon_l$ | liquid porosity |
| $\varepsilon_P$ | volume fraction of persister cells |
| $\varepsilon_{Pa}$ | volume fraction of *Pseudomonas aeruginosa* |
| $\lambda$ | detachment rate coefficient ($m^{-1}$ $day^{-1}$) |
| $\mu_{max}$ | maximum specific growth rate ($day^{-1}$) |
| $\xi$ | dimensionless transformed coordinate |
| $\rho$ | density ($g/m^3$) |

*Subscripts*

| | |
|---|---|
| a | active microbial cells |
| b | biocide |
| d | disinfection |
| EPS | extracellular polymeric substance |
| glu | glucose |
| $i$ | particulate phase components index |
| l | liquid phase |
| o | oxygen |
| p | persister cell |
| Pa | *Pseudomonas aeruginosa* |
| r | reaction |

*Superscript*

| | |
|---|---|
| * | dimensionless variable |

cide treatment; the influence of the variations of the primary variables on the microbial survival is explored. Comprehensive correlations are developed for three microbial survival intervals, namely high, moderate, and low disinfection rates.

## 2. Analysis and methodology

### 2.1. Biofilm

A multispecies model is utilized to account for the microbial cell growth, EPS production, microbial disinfection, persister cell formation, nutrient consumption and biocide reaction. A schematic of the system under consideration, including both the biofilm and the bulk fluid, is shown in Fig. 1. Biofilm consists of particulate and dissolved phases. Particulate phase includes microbial cells and EPS and dissolved phase contains nutrients and biocide. Considering the conservation of mass for the particulate phase with an assumption of dominant bulk motion, explained in Shafahi and Vafai [31], the governing equations for the microbial cells and EPS can be presented as

$$\frac{\partial \varepsilon_i}{\partial t} + \nabla \cdot (u\varepsilon_i) = \frac{r_i}{\rho_i}, \quad i = \mathrm{Pa}, \mathrm{p}, \mathrm{EPS} \tag{1}$$

where $u$ is the expansion velocity of the biofilm matrix. The thickness of the biofilm is changing with time and the governing equations for particulate and dissolved phases are solved in a moving boundary domain.

Reaction terms for particulate phase components can be presented as [1,13,35]:

$$r_{Pa} = \underbrace{\mu_{max}\frac{C_{glu}}{K_{glu}+C_{glu}}\frac{C_o}{K_o+C_o}\varepsilon_{pa}\rho_{pa}}_{\text{growth}} - \underbrace{k_d C_b \varepsilon_{pa}\rho_{pa}}_{\text{disinfection}} - \underbrace{k_{lo}\mu_{max}\frac{C_{glu}}{K_{glu}+C_{glu}}\frac{C_o}{K_o+C_o}C_b\varepsilon_{pa}\rho_{pa}}_{\text{loss/reversion to persister cells}} \tag{2}$$

Regular microbial cell conversion to persister cell occurs based on the following reaction:

$$r_p = \underbrace{k_{lo}\mu_{max}\frac{C_{glu}}{K_{glu}+C_{glu}}\frac{C_o}{K_o+C_o}C_b\varepsilon_{pa}\rho_{pa}}_{\text{conversion to persister cells}} \tag{3}$$

It is assumed that the loss of regular cells to the persister cells depends on the growth rate and biocide concentration. Loss rate coefficient $k_{lo}$ is taken from the work of Cogan [1].

The EPS formation rate occurs based on the following equation [35]:

$$r_{EPS} = i_2 * \underbrace{\left(\mu_{max}\frac{C_{glu}}{K_{glu}+C_{glu}}\frac{C_o}{K_o+C_o}\varepsilon_{pa}\rho_{pa}\right)}_{\text{growth}} \tag{4}$$

where growth and disinfection terms are taken from [15,35] and $i_2$ is a stoichiometric factor ($g_{pa}/g_{EPS}$) as EPS growth is assumed to be proportional to the microbial cell growth.

The non-dimensional form of the particulate phase equations can be presented as:

Pa (regular microbial cells):

$$\frac{\partial \varepsilon_{pa}}{\partial t^*} = \left(\frac{C^*_{glu}}{K^*_{glu}+C^*_{glu}}\frac{C^*_o}{K^*_o+C^*_o}\right)\left(B_{pa,1}\varepsilon_{pa} - B_{pa,2}\varepsilon^2_{pa} - B_{pa,3}C^*_b\varepsilon_{pa}\right) + \left(B_{pa,4}C^*_b\right)\varepsilon^2_{pa} - B_{pa,5}C^*_b\varepsilon_{pa} - B_{pa,6}\frac{\partial \varepsilon_{pa}}{\partial \xi} \tag{5}$$

P (persister cells):

$$\frac{\partial \varepsilon_p}{\partial t^*} = \left(\frac{C^*_{glu}}{K^*_{glu}+C^*_{glu}}\frac{C^*_o}{K^*_o+C^*_o}\right)\left(B_{p,1}\varepsilon_{pa} - B_{p,2}\varepsilon^2_{pa}\right) + \left(B_{p,3}C^*_b\right)\varepsilon^2_{pa} - B_{p,4}\frac{\partial \varepsilon_p}{\partial \xi} \tag{6}$$

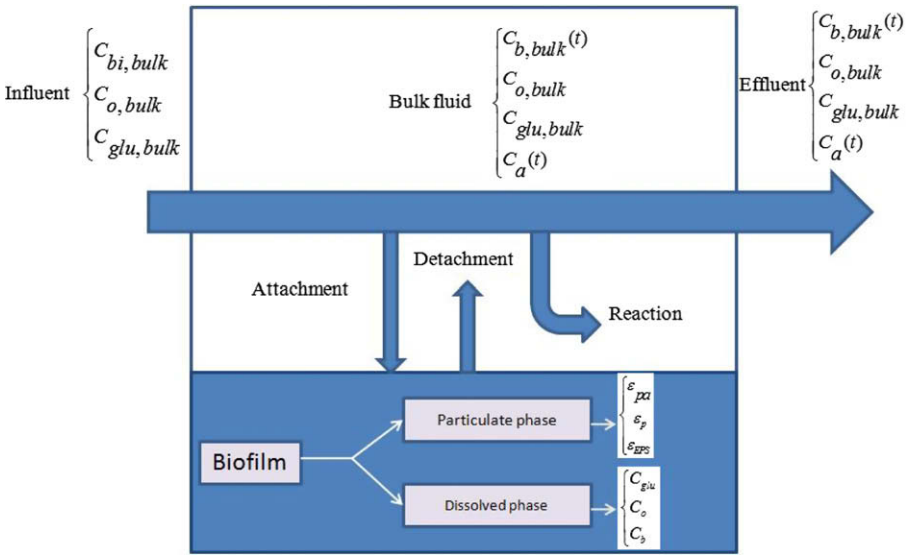


**Fig. 1.** Simple schematic of transport within the biofilm reactor.

EPS (extracellular polymeric substance):

$$\frac{\partial \varepsilon_{\mathrm{EPS}}}{\partial t^*} = \left(\frac{C^*_{\mathrm{glu}}}{K^*_{\mathrm{glu}} + C^*_{\mathrm{glu}}}\frac{C^*_{\mathrm{o}}}{K^*_{\mathrm{o}} + C^*_{\mathrm{o}}}\right)\left(B_{\mathrm{EPS},1}\varepsilon_{\mathrm{pa}} - B_{\mathrm{EPS},2}\varepsilon_{\mathrm{pa}}\varepsilon_{\mathrm{EPS}}\right) + \left(B_{\mathrm{EPS},3}C^*_{\mathrm{b}}\right)\varepsilon_{\mathrm{EPS}}\varepsilon_{\mathrm{pa}} - B_{\mathrm{EPS},4}\frac{\partial \varepsilon_{\mathrm{EPS}}}{\partial \xi} \tag{7}$$

where non-dimensional variables and groups can be presented as:

$$\xi = \frac{x}{L};\quad t^* = \frac{t}{t_{\mathrm{b}}};\quad K^*_{\mathrm{glu}} = \frac{K_{\mathrm{glu}}}{C_{\mathrm{bi,bulk}}};\quad K^*_{\mathrm{o}} = \frac{K_{\mathrm{o}}}{C_{\mathrm{bi,bulk}}};$$
$$C^*_{\mathrm{glu}} = \frac{C_{\mathrm{glu}}}{C_{\mathrm{bi,bulk}}};\quad C^*_{\mathrm{o}} = \frac{C_{\mathrm{o}}}{C_{\mathrm{bi,bulk}}};\quad C^*_{\mathrm{b}} = \frac{C_{\mathrm{b}}}{C_{\mathrm{bi,bulk}}};\quad C^*_{\mathrm{a}} = \frac{C_{\mathrm{a}}}{C_{\mathrm{bi,bulk}}}; \tag{8}$$
$$C^*_{\mathrm{o,bulk}} = \frac{C_{\mathrm{o,bulk}}}{C_{\mathrm{bi,bulk}}};\quad C^*_{\mathrm{glu,bulk}} = \frac{C_{\mathrm{glu,bulk}}}{C_{\mathrm{bi,bulk}}};\quad C^*_{\mathrm{b,bulk}} = \frac{C_{\mathrm{b,bulk}}}{C_{\mathrm{bi,bulk}}};$$

$$B_{\mathrm{pa},1} = t_{\mathrm{b}}\mu_{\max};\quad B_{\mathrm{pa},2} = B_{\mathrm{p},2} = B_{\mathrm{EPS},2} = \frac{t_{\mathrm{b}}\mu_{\max}(1+i_2)}{1-\varepsilon_{\mathrm{l}}};$$
$$B_{\mathrm{pa},3} = B_{\mathrm{p},1} = t_{\mathrm{b}}\mu_{\max}k_{\mathrm{lo}};\quad B_{\mathrm{pa},4} = B_{\mathrm{p},3} = B_{\mathrm{EPS},3} = \frac{t_{\mathrm{b}}k_{\mathrm{d}}C_{\mathrm{bi,bulk}}}{1-\varepsilon_{\mathrm{l}}}; \tag{9}$$
$$B_{\mathrm{pa},5} = t_{\mathrm{b}}k_{\mathrm{d}}C_{\mathrm{bi,bulk}};\qquad B_{\mathrm{pa},6} = B_{\mathrm{p},4} = B_{\mathrm{EPS},4} = t_{\mathrm{b}}\left(\frac{u-\xi u_{\mathrm{l}}}{L}\right);$$
$$B_{\mathrm{EPS},1} = t_{\mathrm{b}}i_2\mu_{\max};$$

where $C_{\mathrm{bi,bulk}}$ is the biocide inlet concentration in the bulk flow and $i_2$ is the stoichiometric coefficient as mentioned earlier.

As nutrients and biocide dissolve in the liquid phase, conservation of mass for dissolved phase components such as glucose, oxygen and biocide which are diffusion dominated [31] can be represented as follows:

$$\frac{\partial(\varepsilon_{\mathrm{l}}C_j)}{\partial t} = r_j + \nabla\cdot(D_j\nabla C_j)\quad j = \mathrm{glu, o, b} \tag{10}$$

Reaction terms for dissolved phase components (glucose, oxygen and biocide) are given as follows [15,35]:

Glucose:

$$r_{\mathrm{glu}} = \left(-\frac{1}{Y_{\mathrm{pa/glu}}} - \frac{i_2}{Y_{\mathrm{eps/glu}}}\right)\left(\mu_{\max}\frac{C_{\mathrm{glu}}}{K_{\mathrm{glu}}+C_{\mathrm{glu}}}\frac{C_{\mathrm{o}}}{K_{\mathrm{o}}+C_{\mathrm{o}}}\varepsilon_{\mathrm{pa}}\rho_{\mathrm{pa}}\right) \tag{11}$$

Oxygen:

$$r_o = \frac{1}{i_1} * r_{\mathrm{glu}} = \frac{1}{i_1}\left(-\frac{1}{Y_{\mathrm{pa/glu}}} - \frac{i_2}{Y_{\mathrm{eps/glu}}}\right)\left(\mu_{\max}\frac{C_{\mathrm{glu}}}{K_{\mathrm{glu}}+C_{\mathrm{glu}}}\frac{C_{\mathrm{o}}}{K_{\mathrm{o}}+C_{\mathrm{o}}}\rho_{\mathrm{pa}}\varepsilon_{\mathrm{pa}}\right) \tag{12}$$

where $Y_{\mathrm{pa/glu}}$ and $Y_{\mathrm{eps/glu}}$ are the observed yield coefficients.

Biocide:

$$r_{\mathrm{b}} = -k_{\mathrm{d}}C_{\mathrm{b}}\rho_{\mathrm{pa}}\varepsilon_{\mathrm{pa}} \tag{13}$$

The dimensionless, transformed version of these equations can be presented as:

$$\frac{\partial C^*_{\mathrm{glu}}}{\partial t^*} = \underbrace{B_{\mathrm{glu},1}\left(\frac{C^*_{\mathrm{glu}}}{K^*_{\mathrm{glu}}+C^*_{\mathrm{glu}}}\frac{C^*_{\mathrm{o}}}{K^*_{\mathrm{o}}+C^*_{\mathrm{o}}}\right)\varepsilon_{\mathrm{pa}}}_{\text{consumption}} + \underbrace{B_{\mathrm{glu},2}\frac{\partial C^*_{\mathrm{glu}}}{\partial \xi}}_{\text{pseudo-convection}} + \underbrace{B_{\mathrm{glu},3}\frac{\partial^2 C^*_{\mathrm{glu}}}{\partial \xi^2}}_{\text{diffusion}} \tag{14}$$

$$\frac{\partial C^*_{\mathrm{o}}}{\partial t^*} = \underbrace{B_{\mathrm{o},1}\left(\frac{C^*_{\mathrm{glu}}}{K^*_{\mathrm{glu}}+C^*_{\mathrm{glu}}}\frac{C^*_{\mathrm{o}}}{K^*_{\mathrm{o}}+C^*_{\mathrm{o}}}\right)\varepsilon_{\mathrm{pa}}}_{\text{consumption}} + \underbrace{B_{\mathrm{o},2}\frac{\partial C^*_{\mathrm{o}}}{\partial \xi}}_{\text{pseudo-convection}} + \underbrace{B_{\mathrm{o},3}\frac{\partial^2 C^*_{\mathrm{o}}}{\partial \xi^2}}_{\text{diffusion}} \tag{15}$$

$$\frac{\partial C^*_{\mathrm{b}}}{\partial t^*} = \underbrace{-B_{\mathrm{b},1}C^*_{\mathrm{b}}\varepsilon_{\mathrm{pa}}}_{\text{disinfection}} + \underbrace{B_{\mathrm{b},2}\frac{\partial C^*_{\mathrm{b}}}{\partial \xi}}_{\text{pseudo-convection}} + \underbrace{B_{\mathrm{b},3}\frac{\partial^2 C^*_{\mathrm{b}}}{\partial \xi^2}}_{\text{diffusion}} \tag{16}$$

The terms called pseudo-convection appear in the equations as a result of coordinate transformation from x to $\xi = \frac{x}{L}$. The transformation is performed to incorporate the effect of moving domain boundary. The dimensionless groups for dissolved phase components are presented as:

$$B_{\mathrm{glu},1} = \frac{t_{\mathrm{b}}\rho_{\mathrm{pa}}\mu_{\max}}{\varepsilon_{\mathrm{l}}C_{\mathrm{bi,bulk}}}\left(-\frac{1}{Y_{\mathrm{pa/glu}}} - \frac{i_2}{Y_{\mathrm{eps/glu}}}\right);\quad B_{\mathrm{o},1} = \frac{B_{\mathrm{glu},1}}{i_1};$$
$$B_{\mathrm{b},1} = \frac{t_{\mathrm{b}}k_{\mathrm{d}}\rho_{\mathrm{pa}}}{\varepsilon_{\mathrm{l}}};$$
$$B_{\mathrm{glu},2} = B_{\mathrm{o},2} = B_{\mathrm{b},2} = \frac{\xi u_{\mathrm{l}}t_{\mathrm{b}}}{L}; \tag{17}$$
$$B_{\mathrm{glu},3} = \frac{D_{\mathrm{glu}}t_{\mathrm{b}}}{\varepsilon_{\mathrm{l}}L^2}\quad B_{\mathrm{o},3} = \frac{D_{\mathrm{o}}t_{\mathrm{b}}}{\varepsilon_{\mathrm{l}}L^2}\quad B_{\mathrm{b},3} = \frac{D_{\mathrm{b}}t_{\mathrm{b}}}{\varepsilon_{\mathrm{l}}L^2}$$

### 2.2. Bulk fluid

Transport equations for active microbial cells and biocide in the bulk fluid are based on the modified version of the work of Stewart et al. [15] and can be presented as:

$$\frac{dC_a}{dt} = \underbrace{\lambda \varepsilon_{pa}|_{x=L}\rho_{pa}L^2\frac{A}{V}}_{\text{detachment from biofilm surface}} + \underbrace{\mu_{max}\frac{C_{glu,bulk}}{K_{glu}+C_{glu,bulk}}\frac{C_{o,bulk}}{K_o+C_{o,bulk}}C_a}_{\text{growth}} - \underbrace{k_d C_{b,bulk}C_a}_{\text{disinfection}} - \underbrace{\frac{Q}{V}C_a}_{\text{outflow}} \tag{18}$$

where $C_a$ is the concentration of active microbial cell in the bulk fluid; $\lambda$, the detachment coefficient; $A$, the biofilm surface area; $V$, the volume of bulk liquid; $C_{b,bulk}$, the biocide concentration in the bulk fluid and $k_d$ is the disinfection coefficient.

The dimensionless equation for the active microbial cell concentration in the bulk fluid can be presented as:

$$\frac{dC^*_a}{dt^*} = B_{a,1}\varepsilon_{pa}|_{\xi=1} + B_{a,2}\left(\frac{C^*_{glu,bulk}}{K^*_{glu}+C^*_{glu,bulk}}\frac{C^*_{o,bulk}}{K^*_o+C^*_{o,bulk}}\right)C^*_a - B_{a,3}C^*_{b,bulk}C^*_a - B_{a,4}C^*_a \tag{19}$$

As can be seen in Fig. 1, some fraction of inlet biocide diffuses to the biofilm surface, some react with the detached cells in the bulk fluid and some exit the reactor. The dimensional and non-dimensional equations for biocide concentration in the bulk fluid are presented as:

$$\frac{dC_{b,bulk}}{dt} = \underbrace{\frac{Q}{V}(C_{bi,bulk}-C_{b,bulk})}_{\text{inflow–outflow}} - \underbrace{k_d C_{b,bulk}C_a}_{\text{disinfection}} - \underbrace{D_b\frac{dC_b}{dx}\Big|_{x=L}\frac{A}{V}}_{\text{attachment}} \tag{20}$$

$$\frac{dC^*_{b,bulk}}{dt^*} = -B_{bb,1}\frac{dC^*_b}{d\xi}\Big|_{\xi=1} + B_{bb,2}\left(1-C^*_{b,bulk}\right) - B_{bb,3}C^*_{b,bulk}C^*_a \tag{21}$$

where $Q$ is the volumetric flow rate. The dimensionless groups in the bulk fluid can be presented as follows:

$$B_{a,1} = t_b\lambda\rho_{pa}\frac{L^2}{C_{bi,bulk}}\frac{A}{V};\quad B_{bb,1} = \frac{t_b D_b}{L}\frac{A}{V};\quad B_{a,2} = t_b\mu_{max};\quad B_{a,3} = B_{bb,3} = t_b k_d C_{bi,bulk};\quad B_{a,4} = B_{bb,2} = t_b\frac{Q}{V} \tag{22}$$

Summary of different physical attributes and dimensionless groups for biofilm and bulk fluid within our model are given in Tables 1–3, respectively.

### 2.3. Numerical solution

Three sets of equations, particulate and dissolved phases as well as bulk fluid, are solved numerically to obtain the biofilm microbial survival rates. At each time step, dissolved phase equations are solved implicitly and the obtained results are employed in particulate phase and bulk fluid equations. The particulate phase and bulk fluid equations are solved explicitly utilizing the dissolved phase solution at a given time step. All equations were discretized using a finite difference method.

Boundary and initial conditions for particulate and dissolved phases can be presented as:

$$\left.\frac{\partial C^*_j}{\partial\xi}\right|_{\xi=0} = 0;\quad \left.\frac{\partial\varepsilon_i}{\partial\xi}\right|_{\xi=0} = 0;\quad C^*_j|_{\xi=1} = C^*_{j,bulk} \tag{23}$$

$$C^*_j(\xi, t=0) = 0;\quad \varepsilon_i(\xi, t=0) = \varepsilon_{i,in} \tag{24}$$

where $\varepsilon_{i,in}$ is the initial value for particulate phase components volume fractions in the biofilm. Glucose and oxygen concentration in the bulk fluid are assumed to be constant. Biocide and active cell microbial concentration are changing with time according to Eqs. (19) and (21).

### 2.4. Microbial cell survival

The microbial survival fraction subject to biocide treatment is defined as follows:

$$s_p = \frac{\rho_a}{\rho^0_a} = \frac{\int_0^L(\varepsilon_{pa}+\varepsilon_p)\,dx}{\left(\varepsilon^0_{pa}+\varepsilon^0_p\right)L_0} \tag{25}$$

where $\rho^0_a$ is the initial density of active cells and $\varepsilon^0_{pa}$ and $\varepsilon^0_p$ are the initial volume fraction of Pa and persister cells, and $L_0$ is the biofilm

**Table 1**
Particulate phase dimensionless groups' categories.

- Particulate phase
  - microbial cell
    - reaction
      - growth: $\mu_{max}\frac{C_{glu}}{K_{glu}+C_{glu}}\frac{C_o}{K_o+C_o}\varepsilon_{pa}\rho_{pa} \Rightarrow B_{pa,1} = t_b\mu_{max}$; $B_{pa,2} = \frac{t_b\mu_{max}(1+i_2)}{1-\varepsilon_i}$;
      - loss to persister cells: $k_{lo}\mu_{max}\frac{C_{glu}}{K_{glu}+C_{glu}}\frac{C_o}{K_o+C_o}C_b\varepsilon_{pa}\rho_{pa} \Rightarrow B_{pa,3} = t_b\mu_{max}k_{lo}$
      - disinfection: $k_d C_b\varepsilon_{pa}\rho_{pa} \Rightarrow B_{pa,5} = t_b k_d C_{bi,bulk}$; $B_{pa,4} = \frac{t_b k_d C_{bi,bulk}}{1-\varepsilon_i}$
    - advective flux: $\rho_{Pa}u \Rightarrow B_{pa,6} = t_b\left(\frac{u-\xi u_l}{L}\right)$
  - Extracellular polymeric substance
    - reaction: $i_2 * \left(\mu_{max}\frac{C_{glu}}{K_{glu}+C_{glu}}\frac{C_o}{K_o+C_o}\varepsilon_{pa}\rho_{pa}\right) \Rightarrow B_{EPS,1} = t_b i_2\mu_{max}$
    - advective flux: $\rho_{EPS}u \Rightarrow B_{EPS,4} = t_b\left(\frac{u-\xi u_l}{L}\right)$

**Table 2**
Dissolved phase dimensionless groups categories.

- Dissolved phase
  - Glucose
    - reaction: $\left(-\frac{1}{Y_{pa/glu}}-\frac{i_2}{Y_{eps/glu}}\right)\left(\mu_{max}\frac{C_{glu}}{K_{glu}+C_{glu}}\frac{C_o}{K_o+C_o}\varepsilon_{pa}\rho_{pa}\right) \Rightarrow B_{glu,1} = \frac{t_b\rho_{pa}\mu_{max}}{\varepsilon_i C_{bi,bulk}}\left(-\frac{1}{Y_{pa/glu}}-\frac{i_2}{Y_{eps/glu}}\right)$
    - diffusive flux: $\nabla\cdot(D_{glu}\nabla C_{glu}) \Rightarrow B_{glu,3} = \frac{D_{glu}t_b}{\varepsilon_i L^2}$
    - pseudo-convection: $\frac{\xi u_l}{L}\frac{\partial(\varepsilon_i C_{glu})}{\partial\xi} \Rightarrow B_{glu,2} = \frac{\xi u_l t_b}{L}$
  - Oxygen
    - reaction: $\frac{1}{i_1}\left(-\frac{1}{Y_{pa/glu}}-\frac{i_2}{Y_{eps/glu}}\right)\left(\mu_{max}\frac{C_{glu}}{K_{glu}+C_{glu}}\frac{C_o}{K_o+C_o}\varepsilon_{pa}\rho_{pa}\right) \Rightarrow B_{o,1} = \frac{B_{glu,1}}{i_1}$
    - diffusive flux: $\nabla\cdot(D_o\nabla C_o) \Rightarrow B_{o,3} = \frac{D_o t_b}{\varepsilon_i L^2}$
    - pseudo-convection: $\frac{\xi u_l}{L}\frac{\partial(\varepsilon_i C_o)}{\partial\xi} \Rightarrow B_{o,2} = \frac{\xi u_l t_b}{L}$
  - Biocide
    - reaction: $k_d C_b\varepsilon_{pa}\rho_{pa} \Rightarrow B_{b,1} = \frac{t_b k_d\rho_{pa}}{\varepsilon_i}$
    - diffusive flux: $\nabla\cdot(D_b\nabla C_b) \Rightarrow B_{b,3} = \frac{D_b t_b}{\varepsilon_i L^2}$
    - pseudo-convection: $\frac{\xi u_l}{L}\frac{\partial(\varepsilon_i C_b)}{\partial\xi} \Rightarrow B_{b,2} = \frac{\xi u_l t_b}{L}$

**Table 3**
Bulk fluid dimensionless groups' categories.

Bulk fluid
- Microbial cell
  - detachment from biofilm surface : $\lambda\varepsilon_{pa}|_{x=L}\rho_{pa}L^2\frac{A}{V}\Rightarrow B_{a,1}=t_b\lambda\rho_{pa}\frac{L^2}{C_{bi,bulk}}\frac{A}{V}$
  - reaction
    - growth : $\mu_{max}\frac{C_{glu,bulk}}{K_{glu}+C_{glu,bulk}}\frac{C_{o,bulk}}{K_o+C_{o,bulk}}C_a\Rightarrow B_{a,2}=t_b\mu_{max}$
    - disinfection : $k_dC_{bi,bulk}C_a\Rightarrow B_{a,3}=t_bk_dC_{bi,bulk}$
  - outflow : $\frac{Q}{V}C_a\Rightarrow B_{a,4}=t_b\frac{Q}{V}$
- Biocide
  - attachment to biofilm surface : $D_b\frac{dC_b}{dx}\Big|_{x=L}\frac{A}{V}\Rightarrow B_{bb,1}=\frac{t_bD_b}{L}\frac{A}{V}$
  - inflow–outflow : $\frac{Q}{V}(C_{bi,bulk}-C_{b,bulk})\Rightarrow B_{bb,2}=B_{a,4}$
  - disinfection : $k_dC_{b,bulk}C_a\Rightarrow B_{bb,3}=B_{a,3}$
- Nutrients
  - Glocose(constant concentration) : $C_{glu,bulk}$
  - Oxygen(constant concentration) : $C_{o,bulk}$

thickness before antibiotic treatment. The microbial survival fraction, $s_p$, will be used to analyze the biofilm's response to changes in the relevant non-dimensional groups described earlier in this work.

### 2.5. Comprehensive correlations

Data is synthesized from well over 630 simulations which account for various physical attributes such as treatment duration ($t_b$), biocide inlet concentration ($C_{bi,bulk}$), disinfection rate coefficient ($k_d$), liquid porosity ($\varepsilon_l$), bulk volumetric flow rate ($Q$), biofilm surface area ($A$) and initial thickness of the biofilm ($L_o$). Square root of survival fraction (SRS) is taken as the output variable to develop the correlations. The presented survival fraction correlations incorporate the effect of persister cells. Since a large number of non-repetitive groups are involved in the model; a backward stepwise regression analysis is performed on the data set to select the most relevant groups. A standard least square method is used to correlate the selected groups by the statistical software JMP 8. Data are divided into three sub-intervals based on the microbial survival fraction. The correlations are categorized into three separate ranges based on the survival fraction. A survival fraction of less than 10% is considered as high disinfection, leading to the first correlation ($SRS_1$); survival fraction between 10% and 40% is considered as moderate disinfection ($SRS_2$); and survival fraction greater than 40% is considered as low disinfection leading to the third correlation ($SRS_3$). Based on the physical understanding of the dominant mechanisms and analysis of the numerical data the three cited sub-regions were found to be the best representation of hundreds of numerical simulations.

The correlation equations for the three intervals can be presented as:

$$\begin{aligned}SRS_1 &= W_0+W_1(t_b\mu_{max})+W_2\left(\frac{t_b\mu_{max}(1+i_2)}{1-\varepsilon_l}\right)\\&+W_3(t_b\mu_{max}k_{lo})+W_4\left(\frac{t_bk_dC_{bi,bulk}}{1-\varepsilon_l}\right)\\&+W_5(t_bk_dC_{bi,bulk})+W_6(t_bi_2\mu_{max})\\&+W_7\left(\frac{t_b\rho_{pa}\mu_{max}}{\varepsilon_lC_{bi,bulk}}\left(-\frac{1}{Y_{pa/glu}}-\frac{i_2}{Y_{eps/glu}}\right)\right)\\&+W_8\left(\frac{D_{glu}t_b}{\varepsilon_lL^2}\right)+W_9\left(\frac{t_bk_d\rho_{pa}}{\varepsilon_l}\right)+W_{10}\left(t_b\frac{Q}{V}\right)\end{aligned}\tag{26}$$

$$\begin{aligned}SRS_2 &= W_0+W_1(t_b\mu_{max})+W_2\left(\frac{t_b\mu_{max}(1+i_2)}{1-\varepsilon_l}\right)\\&+W_3(t_b\mu_{max}k_{lo})+W_4\left(\frac{t_bk_dC_{bi,bulk}}{1-\varepsilon_l}\right)\\&+W_5\left(\frac{t_b\rho_{pa}\mu_{max}}{\varepsilon_lC_{bi,bulk}}\left(-\frac{1}{Y_{pa/glu}}-\frac{i_2}{Y_{eps/glu}}\right)\right)\\&+W_6\left(\frac{D_{glu}t_b}{\varepsilon_lL^2}\right)+W_7\left(\frac{t_bk_d\rho_{pa}}{\varepsilon_l}\right)+W_8\left(t_b\frac{Q}{V}\right)+W_9\left(\frac{t_bD_b}{L}\frac{A}{V}\right)\end{aligned}\tag{27}$$

$$\begin{aligned}SRS_3 &= W_0+W_1\left(\frac{t_bk_dC_{bi,bulk}}{1-\varepsilon_l}\right)+W_2(t_bk_dC_{bi,bulk})\\&+W_3(t_bi_2\mu_{max})\\&+W_4\left(\frac{t_b\rho_{pa}\mu_{max}}{\varepsilon_lC_{bi,bulk}}\left(-\frac{1}{Y_{pa/glu}}-\frac{i_2}{Y_{eps/glu}}\right)\right)\\&+W_5\left(\frac{D_ot_b}{\varepsilon_lL^2}\right)+W_6\left(\frac{D_bt_b}{\varepsilon_lL^2}\right)+W_7\left(t_b\lambda\rho_{pa}\frac{L^2}{C_{bi,bulk}}\frac{A}{V}\right)\\&+W_8\left(t_b\frac{Q}{V}\right)+W_9\left(\frac{t_bD_b}{L}\frac{A}{V}\right)\end{aligned}\tag{28}$$

Correlation coefficients and the average associated errors for each interval are given in Table 4.

## 3. Results and discussion

The numerical results from the present model are compared in Fig. 2 with the experimental data from the work of Anwar et al. [36] where they imposed Pa biofilm under the influence of Piperacillin and Tobramycin in a chemostat system. The physical parameters such as reaction coefficients utilized for this comparison are taken from [1,14,35]. It can be seen that for the first few hours of biocide treatment, there is almost no difference between the curves with and without the effect of persister cells. However, for longer treatment durations the difference between the two curves widens. At the end of treatment duration, there is a substantially larger difference between the survival fractions with and without the persister cells. There is an over estimation for the survival results from our model compared with the experimental data. It can be seen that survival curve for the model without the persister cells results in a better agreement with the experimental data. This might be attributed to the uncertainty in the disinfection and loss coefficients. In their experiments, Anwar et al. [36] used two different types of antibiotics namely piperacillin and tobramycin while in our model we consider the same reaction coefficient for both of these antibiotics. It should also be noted that the Pa bio-

**Table 4**
Correlation coefficients for three intervals of SRS (square root of survival).

| Coefficient | $SRS_1$ survival < 10% | $SRS_2$ 10% ⩽ survival < 40% | $SRS_3$ survival ⩾ 40% |
|---|---|---|---|
| $W_0$ | 0.287923 | 0.524134 | 0.907849 |
| $W_1$ | −0.8222 | −0.67333 | −0.00274 |
| $W_2$ | −0.96362 | −0.07037 | 0.014218 |
| $W_3$ | 358.8926 | 47.16596 | −0.1413 |
| $W_4$ | 0.03531 | 0.007179 | $-8.9\times10^{-7}$ |
| $W_5$ | −0.21762 | $-4.7\times10^{-6}$ | 0.033942 |
| $W_6$ | 0.992957 | $-9.6\times10^{-8}$ | −0.10591 |
| $W_7$ | $-7\times10^{-6}$ | $-4.3\times10^{-6}$ | 74.20954 |
| $W_8$ | $-1.2\times10^{-8}$ | 0.019992 | −0.05416 |
| $W_9$ | $-4.6\times10^{-6}$ | −0.00868 | 0.001607 |
| $W_{10}$ | −0.05725 | – | – |
| Average error | 2.96% | 6.65% | 2.81% |

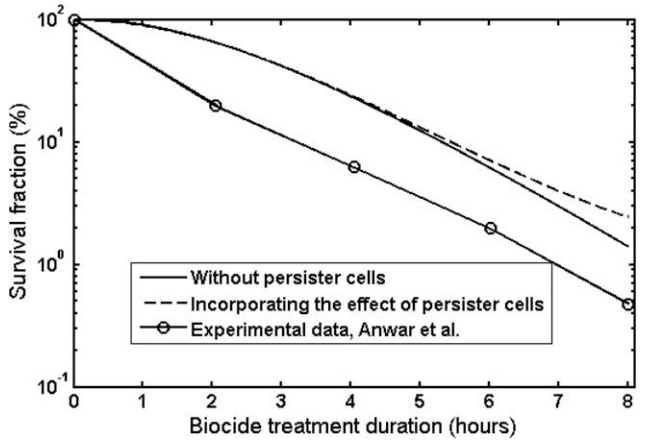


**Fig. 2.** Comparison of microbial survival curves between the current model and the experimental data of Anwar et al. [36] for Pa biofilm exposed to piperacillin ($C_{bi,bulk}$: 505 mg/L; treatment duration: 8 h; 2 days old biofilm; $k_d$: 0.9240 $m^3\ g^{-1}\ day^{-1}$).

film has a heterogeneous structure and a one dimensional representation of the process might not be accurate.

Fig. 3 displays the results of our three correlations together. As seen in Table 4, the average errors for high, moderate and low disinfection sub-regions are relatively small considering the large quantity of correlated data. The effect of biofilm interface velocity on microbial survival fraction for high, moderate and low disinfection regions is shown in Fig. 4. The biofilm response is dependent on the dominance of different mechanisms, during the biocide treatment, within the sub-regions shown in Fig. 4. For the high disinfection region, Fig. 4a, the slope of the curve is negative and the larger absolute value of $u_l$ (interface velocity in the high disinfection sub-interval is negative) leads to a larger microbial survival fraction. The higher interface velocity in this region leads to a faster reduction of biofilm thickness, $L$, when subjected to the biocide treatment. For the high disinfection region, most of the regular cells are deactivated and the majority of the remaining bacteria are persister cells. Based on the survival fraction definition given in Eq. (25), for this sub-region, the effect of an increase in the volume fraction of persister cells is quite substantial leading to a larger survival fraction. For the moderate disinfection region, Fig. 4b, the fraction of persister cells can be quite smaller than the regular cells or comparable to their population depending on the disinfection rate. This is an intermediate region for the biofilm resistance dominant mechanisms against the biocide and there is no clear trend showing the variation of $s_p$ versus the interface velocity. For low disinfection region, Fig. 4c, $u_l$ turns positive. In this region, the microbial survival fraction increases while the disinfection rate decreases. It should be noted that the low disinfection region is characterized by the larger positive values of $u_l$ as opposed to the high disinfection region. It can be observed that the coefficient of persister cells dimensionless group ($B_{p,1}$), given in Table 5, is substantially larger for the high disinfection region, $SRS_1$, compared to moderate disinfection region, $SRS_2$, or the low disinfection region, $SRS_3$, for which the persister cells dimensionless group has not even been selected as an effective contributor.

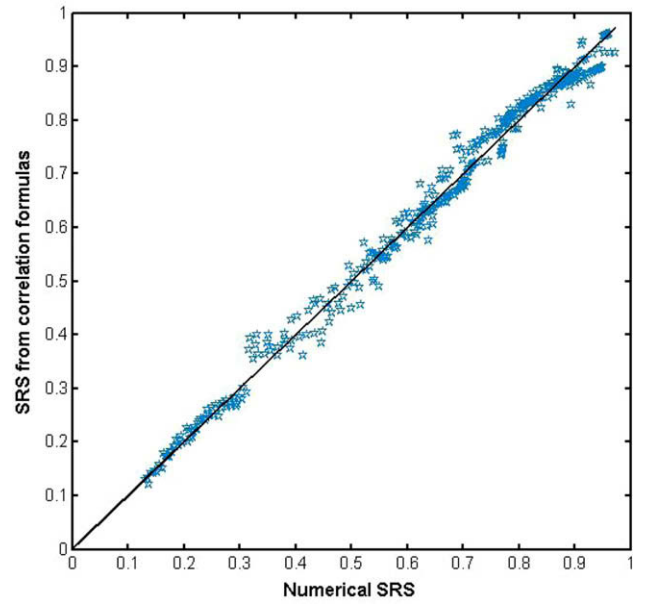


**Fig. 3.** Comparison of the microbial survival from the presented correlations versus the numerical simulations. (survival fractions from all three sets of correlations).

Fig. 5 shows the behavior of diffusional dimensionless groups from the dissolved phase during the treatment process. The three non-dimensional groups, $B_{glu,3}$, $B_{o,3}$, $B_{b,3}$ function similarly with respect to microbial survival fraction. As such, only $B_{b,3}$, is chosen to represent the diffusional characteristics of the dissolved phase. The curve displaying the microbial survival fraction approaches unity when $B_{b,3}$ is close to zero (which is related to the case of no penetration of biocide into the biofilm). As $B_{b,3}$ becomes larger the survival fraction approaches zero which is expected due to a higher diffusional penetration of the biocide into the biofilm. The same trend occurs for glucose and oxygen diffusional dimensionless groups.

Fig. 6 displays the model results incorporating the formation of persister cells compared with the case when they are neglected within the biofilm. The relative difference between the survival fractions with and without persister cells is characterized by $\Delta$ defined as

$$\Delta = \frac{s_p - s_n}{s_p} \tag{29}$$

where $s_p$ is the survival fraction with persister cells and $s_n$ is the survival fraction without the persister cells. The difference between the two models is negligible at the start of the disinfection process when the survival fraction is close to unity. As the regular microbial cells are eradicated, $\Delta$ increases. It can be seen in Fig. 6 that when the biofilm is highly disinfected and the survival fraction of regular cells (other than persister cells) is almost zero; the difference between the two curves increases substantially. In our model it is assumed that persister cells never get disinfected. Therefore, when the survival fraction is close to zero no cells remain within the biofilm except for a very small fraction of persister cells.

Most of the individual dimensionless groups involved in the correlations do not show a clear trend in describing the microbial survival fraction. This is due to the fact that survival is a function of several simultaneous interactions as represented in the given comprehensive correlations. In order to provide an overall insight regarding the contribution of each pertinent dimensionless group in the high, medium and low categories, individual group coefficients are represented in Table 5. It can be seen that for the high disinfection rate ($SRS_1$), reversion to persister cells is pronounced and has a substantially large coefficient. After the role of persister cells microbial growth terms possess the second position. In the moderate disinfection rate ($SRS_2$), persister cells dimensionless group ($B_{p,1}$) still has a dominant effect but not as prominent as the high disinfection case. In the low disinfection rate, $B_{p,1}$ is not even a relevant dimensionless group to correlate the survival fraction. Microbial cells detachment coefficient, $B_{a,1}$, is the largest in the survival correlation. Physically, the detachment effect is important at the low disinfection rates when the biofilm thickness is more significant.

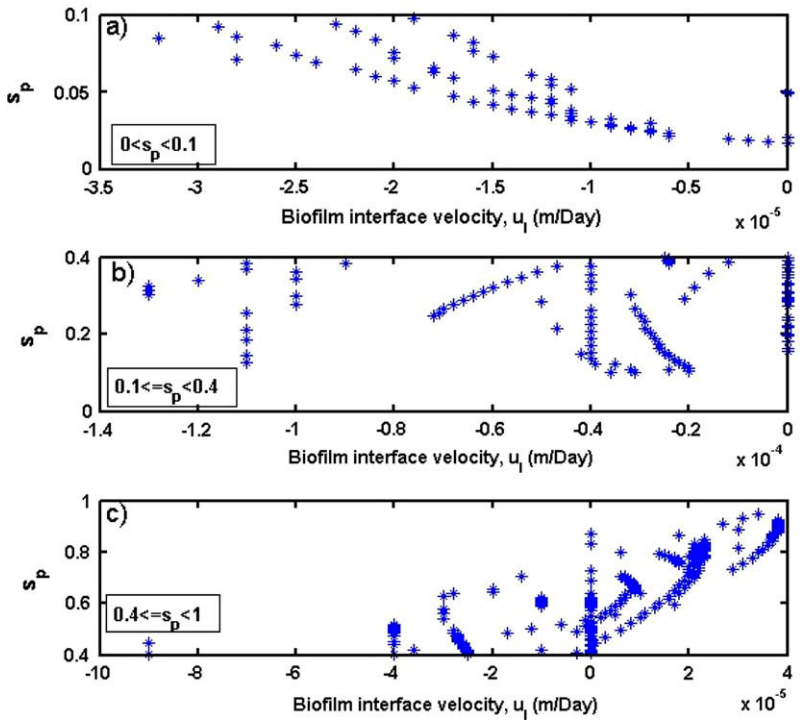


**Fig. 4.** Effect of biofilm interface velocity on microbial survival fraction for three sub-intervals of high, moderate and low disinfection.

**Table 5**
Dimensionless groups coefficients in different correlations.

| Dimensionless groups coefficients | $SRS_1$ high disinfection | $SRS_2$ moderate disinfection | $SRS_3$ low disinfection |
|---|---|---|---|
| $B_{pa,1} = t_b\mu_{max}$ | −0.8222 | −0.67333 | – |
| $B_{pa,2} = \frac{t_b\mu_{max}(1+i_2)}{1-\varepsilon_l}$ | −0.96362 | −0.07037 | – |
| $B_{p,1} = t_b\mu_{max}k_{lo}$ | 358.8926 | 47.16596 | – |
| $B_{pa,4} = \frac{t_b k_d C_{bi,bulk}}{1-\varepsilon_l}$ | 0.03531 | 0.007179 | −0.00274 |
| $B_{pa,5} = t_b k_d C_{bi,bulk}$ | −0.21762 | – | 0.014218 |
| $B_{EPS,1} = t_b i_2 \mu_{max}$ | 0.992957 | – | −0.1413 |
| $B_{glu,1} = \frac{t_b\rho_{pa}\mu_{max}}{\varepsilon_l C_{bi,bulk}}\left(-\frac{1}{Y_{pa/glu}}-\frac{i_2}{Y_{eps/glu}}\right)$ | $-7\times10^{-6}$ | $-4.7\times10^{-6}$ | $-8.9\times10^{-7}$ |
| $B_{glu,3} = \frac{D_{glu}t_b}{\varepsilon_l L^2}$ | $-1.2\times10^{-8}$ | $-9.6\times10^{-8}$ | – |
| $B_{b,1} = \frac{t_b k_d \rho_{pa}}{\varepsilon_l}$ | $-4.6\times10^{-6}$ | $-4.3\times10^{-6}$ | – |
| $B_{o,3} = \frac{D_o t_b}{\varepsilon_l L^2}$ | – | – | 0.033942 |
| $B_{b,3} = \frac{D_b t_b}{\varepsilon_l L^2}$ | – | – | −0.10591 |
| $B_{a,1} = t_b\lambda\rho_{pa}\frac{L^2}{C_{bi,bulk}}\frac{A}{V}$ | – | – | 74.20954 |
| $B_{a,4} = t_b\frac{Q}{V}$ | −0.05725 | 0.019992 | −0.05416 |
| $B_{bb,1} = \frac{t_b D_b}{L}\frac{A}{V}$ | – | −0.00868 | 0.001607 |

## 4. Conclusions

A comprehensive model including disinfection and transport in both the bulk fluid and the biofilm incorporating the dynamic growth of the film and attachment and detachment in the bulk fluid is developed to study the microbial response to the biocide treatment. The results from our model are compared with the available experimental data. Microbial survival is taken as the system response to the biocide treatment. Three comprehensive correlations are developed based on hundreds of numerical simulations incorporating variations in primary parameters such as, treatment duration ($t_b$), biocide inlet concentration ($C_{bi,bulk}$), disinfection rate coefficient ($k_d$), liquid porosity($\varepsilon_l$), bulk volumetric flow rate ($Q$), biofilm surface area ($A$) and initial thickness of the biofilm ($L_0$). Some approaches have been taken to mimic the biofilm resistance against antibiotics [1,12–16]. However, in most of these papers, various aspects considered in this work such as comprehensive modeling of particulates, nutrients, persister cells formation and proper accounting for reaction terms have not been taken into account. To the authors' best knowledge, the current model is the first comprehensive model that considers several physical attributes simultaneously and presents a set of correlations to predict the microbial survival of a biofilm subject to the biocide treatment.

Presentation of the survival fraction in terms of the pertinent dimensionless groups enables us to investigate the simultaneous effect and importance of pertinent physical parameters affecting the biofilm characteristics. Each dimensionless group is a coefficient of a pertinent physical term in the presented model and can be used to study the system response and its sensitivity to the individual changes within the groups. Dominant mechanisms for different survival sub-categories are explored and the signifi-

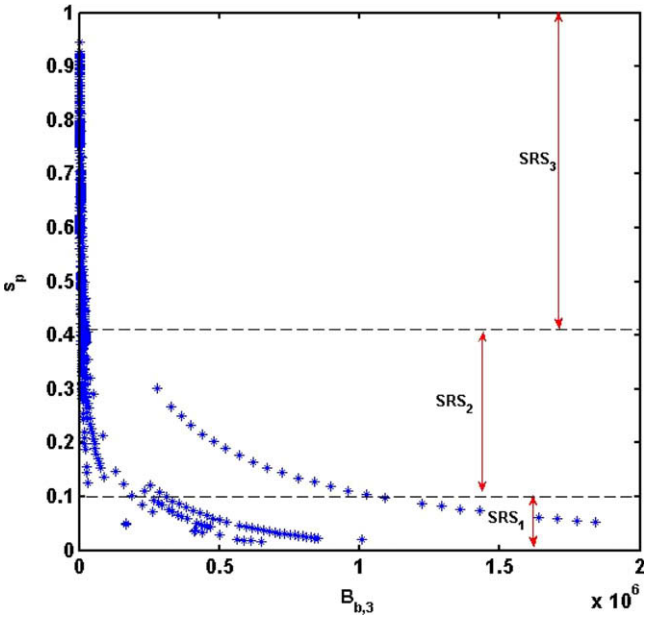


**Fig. 5.** Effect of $B_{b,3}$ on microbial survival fraction for the high, moderate and low disinfection sub-regions.

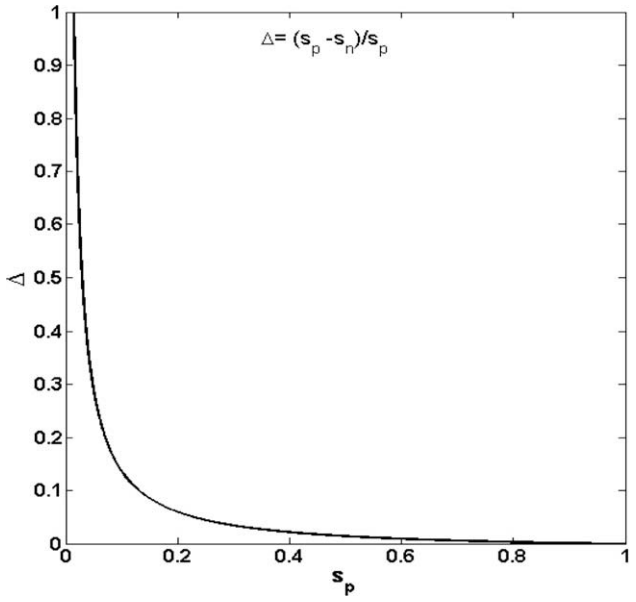


**Fig. 6.** Representation of the relative difference between the survival fractions with and without the persister cells, $\Delta = \frac{s_p - s_n}{s_p}$.

cance of incorporating the effect of persister cells in modeling the survival fraction is studied through assessing the difference between the results of the model which accounts for the presence of persister cells and the one which neglects them. As seen in the correlation results, different mechanisms are dominant depending on the biofilm disinfection rate. It is recommended that aspects related to non-uniform characteristics of the biofilm in response to biocide treatment to be studied in the future.

## References

[1] N.G. Cogan, Effects of persister formation on bacterial response to dosing, J. Theor. Biol. 238 (2006) 694–703.
[2] D. Davies, Understanding biofilm resistance to antimicrobial agents, Nature 2 (2003) 114–122.
[3] Y. Aspa, G. Debenest, M. Quintard, Effective transport properties of porous biofilms, in: Eurotherm Seminar 81, Reactive Heat Transfer in Porous Media, France, June 4–6, 2007.
[4] J.D. Bryers, B.D. Ratner, Biomaterials approaches to combating oral biofilms and dental disease, BMC Oral Health 6 (2006) S15.
[5] J.D. Bryers, Medical biofilms, Biotechnol. Bioeng. 100 (2008) 1–18.
[6] J.W. Costerton, P.S. Stewart, E.P. Greenberg, Bacterial biofilms: a common cause of persistent infections, Science 284 (1999) 1318–1322.
[7] J. Jass, S. Surman, J.T. Walker, Medical Biofilms, Detection, Prevention and Control, Wiley, New York, 2003.
[8] P. Vadgama, Surfaces and Interfaces for Biomaterials, CRC Press, Cambridge, 2005.
[9] J.D. Chambless, S. Hunt, P.S. Stewart, A three-dimensional computer model of four hypothetical mechanisms protecting biofilms from antimicrobials, Appl. Environ. Microbiol. 72 (2006) 2005–2013.
[10] N.G. Cogan, R. Cortez, L. Fauci, Modeling physiological resistance in bacterial biofilms, Bull. Math. Biol. 67 (2005) 831–853.
[11] N.G. Cogan, Two fluid model of biofilm disinfection, Bull. Math. Biol. 70 (2008) 800–819.
[12] M.E. Roberts, P.S. Stewart, Modeling antibiotic tolerance in biofilms by accounting for nutrient limitation, Antimicrob. Agents Chemother. 48 (2004) 48–52.
[13] M.E. Roberts, P.S. Stewart, Modeling protection from antimicrobial agents in biofilms through the formation of persister cells, Microbiology 151 (2005) 75–80.
[14] P.S. Stewart, Biofilm accumulation model that predicts antibiotic resistance of *Pseudomonas aeruginosa* biofilms, Antimicrob. Agents Chemother. 38 (1994) 1052–1058.
[15] P.S. Stewart, M.A. Hamilton, B.R. Goldstein, B.T. Schneider, Modeling biocide action against biofilms, Biotechnol. Bioeng. 49 (1996) 445–455.
[16] P.S. Stewart, Theoretical aspects of antibiotic diffusion into microbial biofilms, Antimicrob. Agents Chemother. 40 (1996) 2517–2522.
[17] N. Bagge, M. Hentzer, J.B. Anderson, O. Ciofu, M. Givskov, N. Hoiby, Dynamics and spatial distribution of β-lactamase expression in *Pseudomonas aeruginosa* biofilm, Antimicrob. Agents Chemother. 48 (2004) 168–1174.
[18] S.S. Sanderson, P.S. Stewart, Evidence of bacterial adaptation to monochloramine in *Pseudomonas aeruginosa* biofilms and evaluation of biocide action model, Biotechnol. Bioeng. 56 (1997) 201–209.
[19] X. Xu, P.S. Stewart, X. Chen, Transport limitation of chlorine disinfection of *Pseudomonas aeroginosa* antrapped in alginate beads, Biotehnol. Bioeng. 49 (1996) 93–100.
[20] K. Lewis, Riddle of biofilm resistance, Antimicrob. Agents Chemother. 45 (2001) 999–1007.
[21] B. Giwercman, E. Jensen, N. Hoiby, A. Kharazmi, J. Costerton, Induction of β-lactamase production in *Pseudomonas aeruginosa* biofilm, Antimicrob. Agents Chemother. 35 (1991) 1008–1010.
[22] B.D. Hoyle, J. Jass, J.W. Costerton, The biofilm glycocalyx as a resistance factor, J. Antimicrob. Chemother. 26 (1990) 1–5.
[23] H. Kumon, K. Tomochika, T. Matunaga, M. Ogawa, H. Ohmori, A sandwich cup method for the penetration assay of antimicrobial agents through *Pseudomonas exopolysaccharides*, Microbiol. Immunol. 38 (1994) 615–619.
[24] I. Keren, N. Kaldalu, A. Spoering, Y. Wang, K. Lewis, Persister cells and tolerance to antimicrobials, FEMS Microbiol. Lett. 230 (2004) 13–18.
[25] C. Von Eiff, Heilmann, G. Peters, New aspects in the molecular basis of polymer-associated infections due to staphylococci, Eur. J. Clin. Microbiol. Infect. Dis. 18 (1999) 843–846.
[26] P.S. Stewart, M.J. Franklin, Physiological heterogeneity in biofilms, Nat. Rev. Microbiol. 6 (2008) 199–210.
[27] N. Sufya, D.G. Allison, P. Gilbert, Clonal variation in maximum specific growth rate and susceptibility towards antimicrobials, J. Appl. Microbiol. 95 (2003) 1261–1267.
[28] K.D. Xu, G.A. Mcfeters, P.S. Stewart, Biofilm resistance to antimicrobial agents, Microbiology 146 (2000) 547–549.
[29] M. Desai, T. Buhler, P. Weller, M. Brwon, Increasing resistance of planktonic and biofilm cultures of *Burkholderia cepecia* to ciprofloxacin and ceftazidime during exponential growth, J. Antimicrob. Chemother. 42 (1998) 153–160.
[30] M.R.W. Brown, D.G. Allison, P. Gilbert, Resistance of bacterial biofilms to antibiotics: a growth-rate related effect?, J Antimicrob. Chemother. 22 (1988) 777–783.
[31] M. Shafahi, K. Vafai, Biofilm affected characteristics of porous structures, Int. J. Heat Mass Transfer 52 (2009) 574–581.
[32] K. Khaled, K. Vafai, The role of porous media in modeling flow and heat transfer in biological tissues, Int. J. Heat Mass Transfer 46 (2003) 4989–5003.
[33] M. Khakpour, K. Vafai, A comprehensive analytical solution of macromolecular transport within an artery, Int. J. Heat Mass Transfer 51 (2008) 2905–2913.
[34] S. Mahjoob, K. Vafai, Analytical characterization of heat transfer through biological media incorporating hyperthermia treatment, Int. J. Heat Mass Transfer 52 (2009) 1608–1618.
[35] O. Wanner, A.B. Cunningham, R. Lundman, Modeling biofilm accumulation and mass transport in a porous medium under high substrate loading, Biotechnol. Bioeng. 47 (1995) 703–712.
[36] H. Anwar, J.L. Strap, K. Chen, W. Costerton, Dynamic interaction of biofilms of mucoid *Pseudomonas aeroginosa* with tobramycin and piperacillin, Antimicrob. Agents Chemother. 36 (1992) 1208–1214.